Generation of multiply charged ions in the context of a vacuum arc thruster

Laurent Garrigues, Pierre Sarrailh

Generation of multiply charged ions in the context of a vacuum arc thruster

IEPC-2022-519

Presented at the 37th International Electric Propulsion Conference
Massachusetts Institute of Technology, Cambridge, MA USA
June 19-23, 2022

L. Garrigues[1]
LAPLACE, Université de Toulouse, CNRS, 118 route de Narbonne, 31062 Toulouse Cedex 9, France

P. Sarrailh[2]
ONERA, Centre de Toulouse, 2 avenue Edouard Belin, 31055 Toulouse Cedex 4, France

Micro vacuum arc thrusters are one of the candidates to be used on board micro and nanosatellites as a propulsion system. They offer several advantages like a high specific impulse, the utilization of a solid propellant with a high density and a small volume that avoids the use of tank and pressure systems, and the expansion of the plasma containing both electrons and ions that dispenses the use of a neutralization cathode. The appearance of multi-charged ions is one of the reason considered to explain the presence of ions at very high velocities. This paper is focused on a simplified one-dimensional model of the vacuum arc thruster considering emissions of electron and atoms at the cathode surface and breakdown of the gas in the inter-electrode gap for typical conditions of a vacuum arc thruster. For a titanium cathode material, results show that stepwise ionization is the key factor to understand the high plasma observed in vacuum arc conditions.

I. Nomenclature

A = Richardson–Dushman (A.m^{-2}.K^{-2})
d = electrode space (m)
E_c = electric field at the cathode (V/m)
E_i = ionization threshold (eV)
e = elementary charge (1.6×10^{-19} C)
ε_0 = free permittivity (F/m)
$\emptyset_{eff}$ = effective work function (V)
k_B = Boltzmann constant (1.38×10^{-23} m^2.kg.s^{-2}.K^{-1})
$k_{rad,Z}$ = Rate constant for radiative recombination (m^3.s^{-1})
$k_{rec,Z}$ = Rate constant for 3 body recombination (m^3.s^{-1})
L = latent heat of evaporation (J. mol^{-1})
λ_i = ionization mean free path (m)
M_a = neutral mass (kg)
N_a = neutral density (m^{-3})
n_e = electron density (m^{-3})
$n_{e,ref}$ = reference electron density (m^{-3})
n_i = ion density (m^{-3})
N_e = number of electrons
P_{atm} = atmospheric pressure (10^5 Pa)

[1] Director of Research at CNRS, LAPLACE, laurent.garrigues@laplace.univ-tlse.fr.
[2] Scientist Researcher, ONERA, pierre.sarrailh@onera.fr.

P_s = saturated vapor pressure (Pa)
R = gas constant = 8.314 $J.K^{-1}.mol^{-1}$
S_{21} = source term ($m^{-2}.s^{-1}$)
σ_i = ionization cross section (m^{-2})
T_{boil} = boiling temperature (K)
T_c = cathode temperature (K)
T_e = electron temperature (K)
V = electric potential (V)
$v_{th,e}$ = electron thermal velocity (m/s)
W_f = work function (V)
Z_i = ion charge state

II. Introduction

The typical missions that microsatellites are (or will be) able to fulfill in the next years are related to space-based science (earth science, weather prediction, astronomy, etc.), commercial (collecting informations for agriculture support by reducing the risk of climatic dramatic changes, finding hidden natural resources, real time imagery, adapt communication network, etc.) and military (real time surveillance, space control, and protection again missile attacks) applications (e.g. [1]). The success of these missions requires complex maneuvers (de-orbiting, orbit raising, flying formation and precise attitude control). The use of micropropulsion systems adapted to the specific requirements of microsatellites is a key point to accomplish the tasks cited above. Critical issues are related to limitations related to weight and volume associated to the satellite platforms. Also, the low level electrical power available onboard small satellites makes the use of pulsed systems preferable [2], [3]. One of the candidate is the so-called Vacuum Arc Thruster (VAT) [4].

Vacuum arcs (also called cathodic arcs) have been extensively studied for various applications: coating, circuit breaker, etc. Vacuum arcs are based on the generation of an arc discharge through the ionization of the vapor neutrals resulting from the evaporation of a cathode metal brought at a high temperature and the emission of electrons from the cathode surface. The discharge takes place in very thin localized area of the cathode (micrometer size) called cathodic spot that changes continuously in time (see Refs [5], [6] for more details). Typical currents are in the range of 100 A to 1 kA and arc voltage between 10 and 100 V. In VAT, the thrust is furnished by the plasma expansion making useless the utilization of a neutralizer. Several companies worldwide currently Alameda Applied Sciences Corporation, United States of America [7], Neumann Space, Australia [8], Space Plasmatics, Israel [9], and Comat Aerospace, France [10], have taken the opportunity to promote VATs as propulsion systems for micro-satellites. In parallel research activities in academic laboratories, for example at the University of Bundeswehr [11] and Georges Washington University [12], are still ongoing to characterize and understand the operation of VATs. The PJP (Plasma Jet Pack) H2020 project aims to group the efforts of Comat Aerospace, research laboratories (CNRS with LAPLACE and ICARE laboratories, Bundeswehr University of Munich), PlasmaSolve and main contractors (OHB Sweden and Thales Alenia Space) to increase thruster performance as well as a deeply improve the understanding of the engine operation [13].

One of the main characteristics of vacuum arc is the presence of multiply charged ions. This has been documented in the literature through experimental works, mainly from measurements of ion time of flight with mass spectrometer (e.g. [14], [15]). Typical mean ion charge varies between 1 and 3 (with ion charge state until 6) depending of the nature of the cathodic material. The application of an external magnetic field as well as a higher discharge current can also influence the mean ion charge state of the discharge [6]. First attempts using a freezing model assuming a thermodynamic local equilibrium in the vicinity of the cathode and that ionization and recombination are balanced meaning that the ion charge state density can be determined from Saha equations have been proposed to explain the measured ion mean charge. The calculations have revealed that this simple approach was only able to reproduce at some extends the measurements. This model has been later completed by including the stepwise ionization region and the fact that not all the ion species are frozen at the same time. This second approach requires the separation of ionization and recombination processes (more details can be found in Ref. [6]). In the context of VAT, the discharge current can reach several kA during a typical duration of 15 μs [16]. Typical same experimental conditions but for a different context has shown that multiply charged metal ions with charge states greater than 10+ can be generated [17]. The generation of highly charged states is one of the reasons put forward to understand the very high velocities reached by the VAT [17]. The goal of this paper is to propose a one-dimensional Hybrid-Monte Carlo-PIC to analyze the generation of multiply charged ions model in the context of VAT for a cathode material made in titanium.

The rest of the paper is organized as the following. In section III, we describe the numerical model hypothesis and equations. Section IV is devoted to the titanium input data necessary for electron and neutral atom mechanisms generation. Section V presents and discusses the simulation results. Section VI summarizes the main conclusion.

III. Description of the Hybrid-Monte-Carlo model

The discharge is modeled through a Hybrid-Monte-Carlo (H-MC) approach. The electron population is separated in two, a first population corresponding to bulk low-energetic electrons which are trapped by the ambipolar electric field and a second population corresponding to high enough energetic electrons to ionize the neutral atoms. For the first population, the ramp of electric potential quickly changes such that the electron mean velocity tends to be negligible compared to drift and diffusion terms. The electron density is in equilibrium with the electric potential and determined from the Maxwell-Boltzmann (MB) equation. The second population responsible for ionization is treated with a Monte Carlo procedure. Heavy species transport is treated with a PIC-like particle model. The plasma is not assumed quasineutral and the self-consistent electric potential is solved from Poisson's equation. Collisions between species are treated with Direct Simulation Monte Carlo (DSMC) method. This model has been successfully used in the context of breakdown in vacuum circuit breakers [18].

The MB relation link the electron density n_e to the electric potential V:

$$n_e = n_{e,ref} \exp[eV/k_B T_e] \quad (1),$$

Where e, k_B, and T_e are elementary charge, Boltzmann constant and electron temperature, respectively. In Eq. (1), $n_{e,ref}$ is the reference electron density taken at the anode where V = 0. The reference electron density is calculated from the integration of the continuity equation between the two electrodes, assuming Maxwellian electrons:

$$\frac{\partial N_e}{\partial t} + \frac{1}{4} n_{e,ref} \mathrm{v}_{th,e} \left[\exp\left(\frac{eV_c}{k_B T_e}\right) + 1\right] = S_{21} \quad (2),$$

Where $N_e = p n_{e,ref}$, with $p = \int_0^d \exp[eV/k_B T_e] dx$, the space integration is made between the inter-electrode space noticed d. The thermal velocity for Maxwellian electrons of mass m_e is given by $\mathrm{v}_{th,e} = \sqrt{8k_B T_e/\pi m_e}$. The first term of left-hand side of Eq. (2) is the time derivative of the number of electrons variation, the second term of left-hand side is simply the balance of flux of electrons between cathode and anode (V_c is the time varying electric potential at the cathode and the electric potential at the anode is fixed to 0). The term of the right-hand side is the generation of the population of bulk electrons (population 1) coming from Monte Carlo electron population (population 2, see below). For a constant electron temperature, fixed to 1 eV in the calculations shown in section V, resolving Eq. (2) at each time step permits to calculate $n_{e,ref}$ and the electron density profile n_e from Eq. (1).

A particle description is used for hot electrons, ions, both assumed un-magnetized, and neutrals. Newton's laws are integrated using a classical leap-frog scheme [19] in which the electric force acts on charged particles and is equal to zero for neutrals. The electric potential is solution of the Poisson's equation:

$$\Delta V = -\frac{e}{\varepsilon_0}[Z_i n_i - n_e] \quad (3),$$

Where ε_0 is the free permittivity and Z_i is the ion charge state.

Neutral-neutral and ion-neutral collisions are included via a DSMC procedure already employed in the context of vacuum circuit breaker [20]. For neutral-neutral collisions, constant variable hard sphere (VHS) cross sections are taken from Ref. [21]. Regarding ion-neutral collisions, only charge exchange collisions are considered and, due to lack of data, same cross sections than for Cu-Cu^+ collisions have been taken for preliminary concerns [20].

IV. Particle generation mechanisms

Important mechanisms occur at the cathode which is maintained at a high temperature during the arc discharge. The first phenomenon is the emission of electrons from the surface. This net emission current density is obtained from the Richardson-Dushman thermionic emission law including the Schottky effect (called field enhanced thermionic emission). The Richardson-Dushman law relies the net emission of electrons from a cathodic material to the temperature T_c at the surface and the electron work function W_f. This relation indicates that for high enough

temperature, the electrons whose energy is closed to the Fermi level have a certain probability to be extracted from the conduction band. The Schottky effect indicates the emission can be enhanced by a local high electric field. The field enhanced thermionic emission is given by [6]

$$J_{em} = AT_c^2 \exp\left(-\frac{e\emptyset_{eff}}{k_B T_c}\right) \quad (4),$$

Where A is constant that is fitted from experimental results. For an current density expressed in A.m^{-2}, the A constant for titanium is 6×10^5 A.m^{-2}.K^{-2} [6]. The effective work function $\emptyset_{eff}$ is given by:

$$\emptyset_{eff} = W_f - \sqrt{\frac{eE_c}{4\pi\varepsilon_0}} \quad (5).$$

The electron work function for titanium is 4.33 V [6]. In Eq. (5), E_c is the electric field in front of the cathode. Eq. (5) is only valid when the second term is a correction of the electron work function. Typically, to be valid, E_c has to be lower than 10^9 V/m (which is the case in our problem as far we did not considered micro-protrusions that can locally enhance the electric field). Remark that when this condition is not satisfied, alternative methods that consists in separating the two contributions are possible and details in Ref. [6].

One other mechanism is the emission of electrons under ion and neutral impacts on the cathode surface. Two types of emission can exist. The first one is the potential emission where electrons can pass the potential barrier by the tunnel effect to neutralize the ion charge particle approaching the surface. For a metal with a first level of ionization E_i, the condition that must be fulfilled is $E_i > 2eW_f$ [22]. Since for titanium E_i = 6.83 eV, this condition in not fulfilled. Only the kinetic emission under heavy species take place and assumed independent of charge or not of the particle, only the energy of the incident particle counts. If measurements of the electron emission yield exist for energies beyond few keV [23], no consolidated values are available in the literature for lower energies. Semi empirical formula based on linear extrapolation are most of time used. We have made calculations testing different electron emission yield for reasonable variations, calculations show that it contributes to less than 1 % to the total electron emission current density at the surface. No reflection mechanisms of electron are considered.

Associated to the emission of electrons, neutral atoms are also emitted from the cathode surface. The flux of neutral atoms is given from the

$$\Gamma_{a,evap} = \frac{P_s}{\sqrt{2\pi M_a k_B T_c}} \quad (6),$$

where M_a is the mass of the evaporated atoms (M_a = 8×10^{-26} kg for titanium), and the saturated vapor pressure P_s can be expressed as a function of latent heat of evaporation L equals to 421 kJ.mol^{-1}, the gas constant R = 8.314 J.K^{-1}.mol^{-1} and the boiling temperature T_{boil} equals to 3560 K for titanium:

$$P_s = P_{atm} \exp\left[-\frac{L}{R}\left(\frac{1}{T_C} - \frac{1}{T_{boil}}\right)\right] \quad (7).$$

The electron-neutral collisions which are considered are stepwise ionizations, elastic and excitation. Cross sections are taken from Quantemol database for elastic and excitation processes [24] and from Ref. [25] for stepwise ionization (see figure 1). Direct ionizations from ground states were not taken into account due to lack of data. For typical cathode temperature T_c of 3200 K and neutral density $N_a \sim 10^{23}$ m^{-3}, the ionization mean free path defined as $\lambda_i = 1/N_a\sigma_i$ is between 10 to 100 μm for electron energies in the range of 10 to 200 eV, to be compared to the typical distance between cathode and anode of ~ 1 cm.

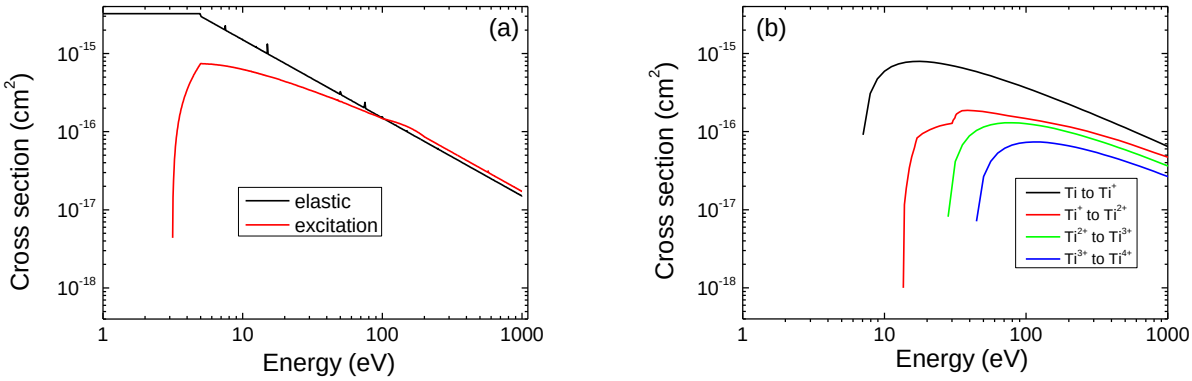

Figure 1. Electron-neutral cross sections for titanium (a) elastic and excitation, (b) stepwise ionization processes.

V. Results and discussion

Calculations have performed for a gap between cathode and anode of 8 mm, the cathode temperature has been chosen such that the calculated plasma density is between 10^{23} to 10^{24} m^{-3} corresponding to typical measured ones [26]. In the calculations, the cathode temperature is assumed constant during the arc phase and fixed to 3200 and 3500 K, the neutral current density being 2.7×10^7 A/m^2 and 10^8 A/m^2, respectively. The electron temperature is fixed to 1 eV. Before the arc takes place, a triggering electrode with a high voltage peak system is used during typically 1 μs. As the initial conditions, in the simulations, we have evaporated neutrals from the surface to start with an initial profile of neutral density. The initial plasma density is 10^{21} m^{-3} (with only single charged ions) The anode potential is at zero and a ramp of voltage is applied on the cathode (see figure 3) during the arc phase.

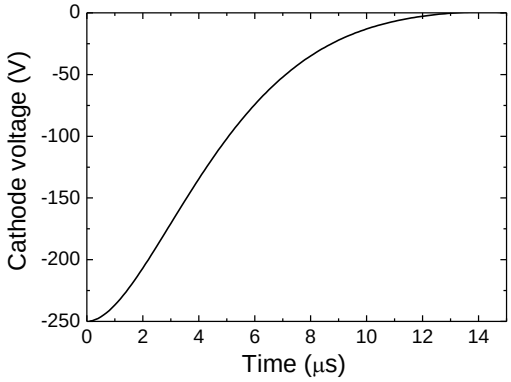

Figure 2. Ramp of voltage.

Comparisons between calculations for a cathode temperatures of 3200 and 3500 K about emission currents, ion charge states and space averaged plasma density are shown in figure 3. In figure 3a, we clearly see that an increase of the cathode temperature leads to an increase of thermionic emission because both of the increase of temperature but also of the electric field strength closed to the cathode. We note that the profile of thermionic emission follows the one of the electric field at the cathode (with a maximum strength reaching few times 10^8 V/m for T_c = 3500 K). The magnitude of electric field strength reached makes the Richardson-Dushman law considering a field-enhanced thermionic emission applicable. As expected, the electron emission under heavy species impacting on the cathode surface is negligible. The higher electric field at the cathode at 3500 K is the consequence of a larger plasma density in the sheath region making the sheath thickness thinner and, as a result, the electric field much higher. The averaged plasma density and the ion charge state Z_i are plotted in Figure 3b. The maximum of plasma density increases by typically one order of magnitude when the temperature passes from 3200 to 3500 K. The ion charge state is maximum after 4 μs for both cases but the magnitude is larger than 2.2 for 3500 K while at a lower temperature it remains close to 1.2. The position of the maximum of both quantities is the same.

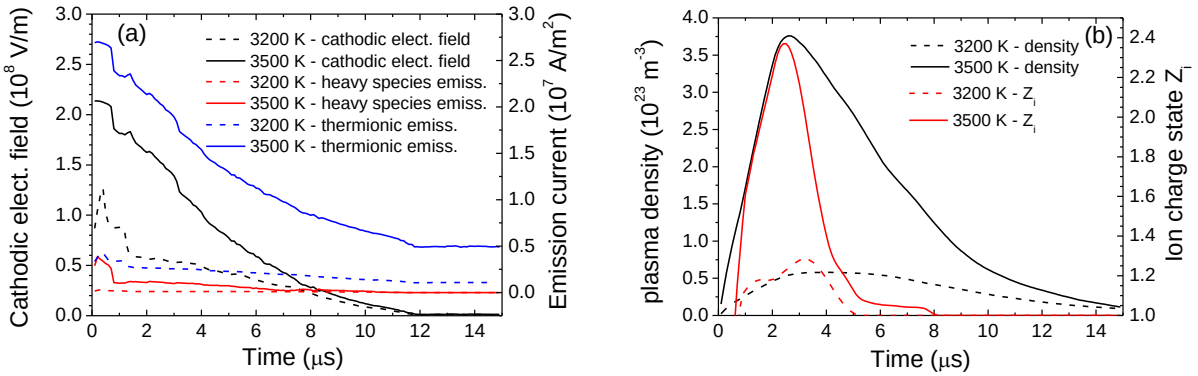

Figure 3. Space averaged profiles of (a) cathodic electric field and electron current density emitted at the surface, (b) plasma density and ion charge state Z_i.

For a cathode temperature of 3500 K we show in figure 4 the space and time profiles of neutral and plasma densities, and ion charge state. We see a strong ionization of the neutral density until 4 μs, the plasma density can reach 8.4×10^{23} m^{-3} (which is typically the same density as the initial neutral density, see below). Electrons emitted at the cathode surface by the field-enhanced thermionic emission gain energy in the sheath to reach a breakdown of the gas. The maximum is located in front of the cathode where the maximum of electron energy is located. After typically 4 mm, the electron energy decreases increasing the ionization mean free path. Note only singly charged ions are produced but the stepwise ionizations lead to the production of higher charge states, mainly $Z_i = 2$ and 3, $Z_i = 4$ staying negligible. Between 4 and 6 μs, a small fraction of higher charge states exits but the kinetic energy of electrons is too low to reach higher levels of charge states. Above 8 μs, the ionization of the neutral atoms is less intense because the emission of the electrons is largely reduced. The plasma density is on the order or below 10^{21} m^{-3}.

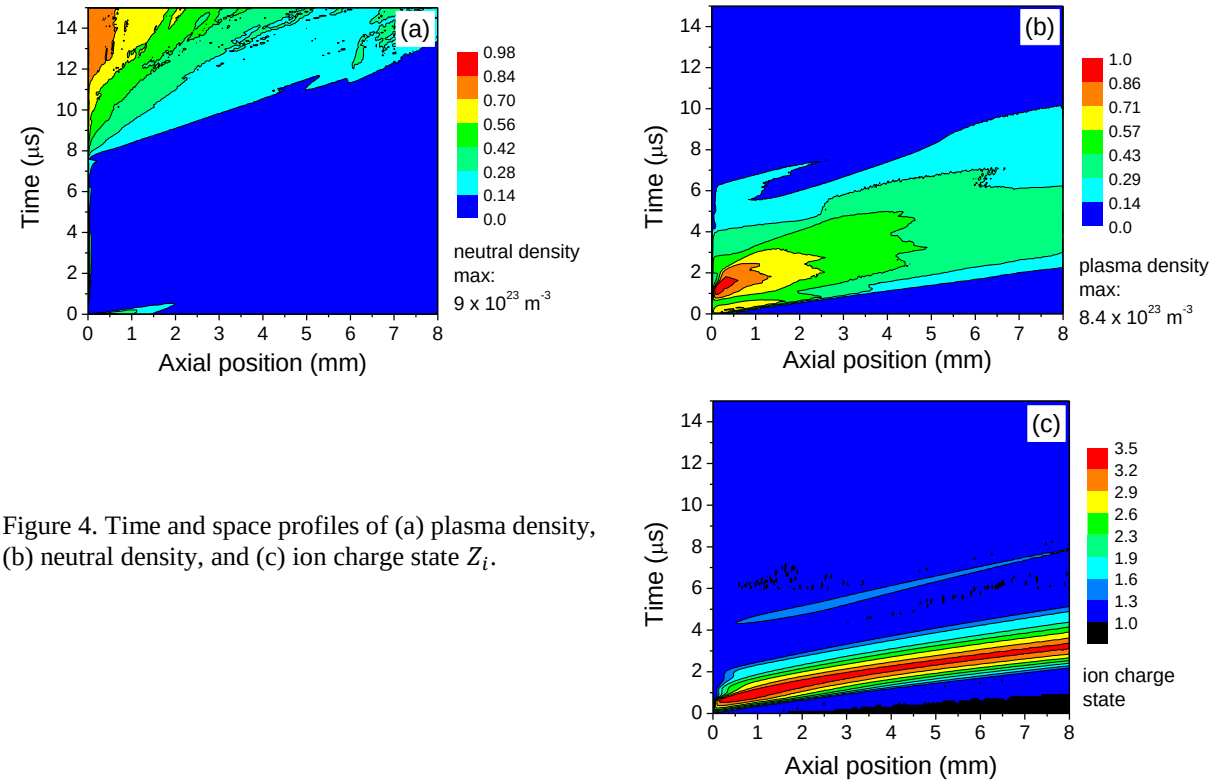

Figure 4. Time and space profiles of (a) plasma density, (b) neutral density, and (c) ion charge state Z_i.

The results of figure 4 shown that the plasma density can be larger than 10^{23} m^{-3}. There are recombination processes that are likely to occur. The first process is the radiative recombination, $Ti^Z + e \xrightarrow[k_{rad,Z}]{} Ti^{Z-1} + h\upsilon$, but the probability is small, compared to the electron-ion three body recombination process $e + e' + Ti^Z \xrightarrow[k_{rec,Z}]{} Ti^{Z-1} + e''$, as far as the plasma density is greater than 3×10^{19} m^{-3} for an electron temperature of 1 eV [27]. In the reaction above, e and e' are low energetic electrons, and e'' a high energetic electron that takes the difference of ionization threshold between Z and $Z-1$. Cao *et al*. have included the electron-ion three body recombination processes through constant rates in the context of copper vacuum arcs [28].

VI. Conclusions and future works

A one-dimensional hybrid model of vacuum arcs has been developed and applied to the case of a titanium cathode surface. Results show that, as observed in many studies of vacuum arcs, the ion charge state can be larger than 1 with the presence of doubly and triply charged ions due to stepwise ionizations, leading to high plasma density ~ 9×10^{23} m^{-3}. Nevertheless, the high level of the plasma density must be taken with caution since no recombination processes have actually been considered.

The initial parameters have been taken from the experimental campaign of the vacuum arc thruster tested at Comat Aerospace, France. A parametric study now must be performed to analyze for example the effect of ramp voltage and triggering time. The change of the cathodic material for which the data are available will be performed. Especially, for materials like zirconium and for some specific conditions, contrary to the case of titanium, the electron-to-neutral current emission ratio becomes larger than one. This specific condition would certainly induce a plasma behavior different from what we have observed in the study presented in this paper.

Acknowledgments

This project has received funding from the European Union's Horizon 2020 research and innovation programme under grant agreement N° 870444, Plasma Jet Pack project. The authors thank Mathieu Masquere and Flavien Valensi, from LAPLACE, Toulouse, France, for sharing preliminary results about the electron density and temperature measurements.

References

[1] A. Camps, "Nanosatellites and Applications to Commercial and Scientific Missions", in *Satellites Missions and Technologies for Geosciences*, edited by V. Demyanov and J. Becedas, IntechOpen (2019).

[2] I. Levchenko *et al*., "Space Micropropulsion Systems for Cubesats and Small Satellites: From Proximate Targets to Furthermost Frontiers", Applied Physics Reviews **5**, 011104 (2018).

[3] W. P. Wright and P. Ferrer, "Electric Micropropulsion Systems", Progress in Aerospace Sciences **74**, 48 (2015).

[4] J. Kolbeck, A. Anders, I. I. Beilis, and M. Keidar, "Micro-Propulsion Based on Vacuum Arcs", Journal of Applied Physics **125**, 220902 (2019).

[5] R. L. Boxman, D. M. Sanders, and P. J. Martin, "Handbook of Vacuum Arc Science and Technology: Fundamentals and Applications", Noyes Publications, 1995.

[6] A. Anders, "Cathodic Arcs: From Fractal Spots to Energetic Condensation", Springer, 2008.

[7] M. Krishnan, K. Velas, and S. Leemans, "Metal Plasma Thruster for Small Satellites", Journal of Propulsion and Power **36**, 535 (2020).

[8] P. Neumann, T. Cullum, A. Bish, A. Doucet, and K. Kanawaka, "Demonstration of Exhaust Plume Quasi-neutrality in a Pulsed Cathodic Arc Thruster", *72nd International Astronautical Congress*, October 2021, Dubai, United Arab Emirates.

[9] S. Chowdhury and I. Kronhaus, "Characterization of Vacuum Arc Thruster Performance in Weak Magnetic Nozzle", Aerospace **7**, 82 (2020).

[10] A. Blanchet, L. Herrero, L. Voisin, B. Pilloy, and D. Courteville, "Plasma Jet Pack Technology for Nano Microsatellites", *36th International Electric Propulsion Conference*, Vienna, Austria, 2019, paper IEPC-2019-271.

[11] M. Kühn, C. Toursel, and J. Schein, "Thrust Measurements on the High Efficient and Reliable Vacuum Arc Thruster (HERVAT)", Applied Science **11**, 2274 (2021).

[12] D. Zolotukhin, K. Daniels, and M. Keidar, "Discharge Characteristics of Two-stage Micro-Cathode Arc MPD Thrusters with a Permanent Magnet and a Pulsed Magnetic Field", Journal of Physics D: Applied Physics **54**, 015201 (2021).

[13] PJP Plasma Jet Pack H2020 project website, https://plasmajetpack.com/.

[14] I. G. Brown, "Vacuum Arc Ion Sources", Review of Scientific Instruments **65**, 3061 (1994).

[15] A. Anders and G. Yu. Yushkov, "Ion Flux from Vacuum Arc Cathode Spots in the Absence and Presence of a Magnetic Field", Journal of Applied Physics **91**, 4824 (2002).

[16] A. Blanchet, L. Herrero, and L. Voisin, "2D Mapping of Vacuum Arc Thruster Plume Plasma Parameters", *35th International Electric Propulsion Conference*, Atlanta, GE, 2017, paper IEPC-2017-574.

[17] G. Yu. Yushkov, A. G. Nikolaev, V. P. Frolova, E. M. Oks, A. G. Rousskikh, and A. S. Zhigalin, "Multiply Charged Metal Ions in High Current Pulsed Vacuum Arcs", Physics of Plasmas **24**, 123501 (2017).

[18] P. Sarrailh, L. Garrigues, G. J. M. Hagelaar, and J. P. Boeuf, "Modeling of breakdown during the post-Arc phase of a vacuum circuit breaker", Plasma Sources Sciences and Technology **19**, 065020 (2010).

[19] J. P. Verboncoeur, "Particle Simulation of Plasmas: Review and Advances", Plasma Physics and Controlled Fusion **47**, A231 (2005).

[20] P. Sarrailh, L. Garrigues, G. J. M. Hagelaar, J. P. Boeuf, G. Sandolache, and S. Rowe, "Sheath Expansion and Plasma Dynamics in the Presence of Electrode Evaporation: Application to a Vacuum Circuit Breaker", Journal of Applied Physics **106**, 053305 (2009).

[21] J. Fan, I. D. Boyd, and C. Shelter, "Monte Carlo Modeling of YBCO Vapor Deposition", AIP Conference Proceedings **585**, 214 (2001).

[22] S. Y. Lai, A. Brown, J. C. Vickerman, and D. Briggs, "The Relationship Between Electron and Ion Induced Secondary Electron Imaging: A Review with New Experimental Observations," Surface and Interface Analysis **8**, 93 (1986).

[23] A. Anders and G. Yu. Yushkov, "Measurements of Secondary Electrons Emitted from Conductive Substrates under High-Current Metal Ion bombardment", Surface and Coatings Technology **136**, 111 (2001).

[24] J. Tennyson, S. Rahimi, C. Hill, L. Tse, A. Vibhakar, D. Akello-Egwel, D. B. Brown, A. Dzarasova, J. R. Hamilton, and D. Jaksch, "QDB: A New Database of Plasma Chemistries and Reactions", Plasma Sources Science and Technology **26**, 055014 (2017).

[25] M. A. Lennon, K. L. Bell, H. B. Gilbody, J. G. Hughes, A. E. Kingston, M. J. Murray, and F. J. Smith, "Recommended Data on the Electron Impact Ionization of Atoms and Ions: Fluorine to Nickel", Journal of Physical and Chemical Reference Data **17**, 1285 (1988).

[26] F. Valensi and M. Masquere, personal communication (2022).

[27] Yu. P. Raizer, "Gas Discharge Physics", Springer-Verlag, 1987.

[28] Z. Cao, R. Li, Z. Wang, B. Cao, Z. Zhou, L. Sun, Y. Geng, and J. Wang, "Three-Dimensional Hybrid Plasma Modeling of Anodic Sputtering in Vacuum Arcs", Plasma Sources Science and Technology **30**, 105020 (2021).

[29] P. Chapelle, J. P. Bellot, A. Jardy, and D. Ablitzer, "Use of kinetic Simulations for the Determination of Particle and Energy Fluxes at the Cathode Surface of a Vacuum Arc", The European Physical Journal: Applied Physics **34**, 43 (2006).